

# Effect of Coloring With Various Metal Oxides on the Microstructure, Color, and Flexural Strength of 3Y-TZP

K. Shah,<sup>1</sup> J. A. Holloway,<sup>2</sup> I. L. Denry<sup>2</sup>

<sup>1</sup> Removable Prosthodontics, Advanced Prosthodontics, Biomaterials, and Hospital Dentistry, UCLA School of Dentistry, Los Angeles, California 90095-1668

<sup>2</sup> College of Dentistry, Section of Restorative and Prosthetic Dentistry, The Ohio State University, Columbus, Ohio 43218-2357

Received 12 February 2007; revised 14 December 2007; accepted 4 February 2008

Published online 23 April 2008 in Wiley InterScience (www.interscience.wiley.com). DOI: 10.1002/jbm.b.31107

**Abstract:** The purpose of this study was to investigate the effect of cerium and bismuth coloring salts solutions on the microstructure, color, flexural strength, and aging resistance of tetragonal zirconia for dental applications (3Y-TZP). Cylindrical blanks were sectioned into disks (2-mm thick, 25-mm in diameter) and colored by immersion in cerium acetate (CA), cerium chloride (CC), or bismuth chloride (BC) solutions at 1, 5, or 10 wt %. The density, elastic constants, and biaxial flexural strength were determined after sintering at 1350°C. The crystalline phases were analyzed by X-ray diffraction before and after aging in autoclave for 10 h. The results showed that the mean density of the colored groups was comparable with that of the control group ( $6.072 \pm 0.008 \text{ g/cm}^3$ ). XRD confirmed the presence of tetragonal zirconia with a slight increase in lattice parameters for the colored groups. A perceptible color difference was obtained for all groups ( $\Delta E^* = 2.57 \pm 0.48$  to  $14.22 \pm 0.98$ ), compared with the control. The mean grain size increased significantly for the groups colored with CC or CA at 10 wt %, compared with the control group ( $0.318 \pm 0.029 \text{ mm}$ ). The mean biaxial strength of CA1%, CA5%, and BC1% groups was not significantly different from that of the control group ( $1087.5 \pm 173.3 \text{ MPa}$ ). The flexural strength of all other groups decreased linearly with increasing concentration for both cerium salts ( $860.7 \pm 172$  to  $274.4 \pm 67.3 \text{ MPa}$ ). The resistance to low temperature degradation was not affected by the coloring process. Coloring with cerium or bismuth salts produced perceptible color differences even at the lowest concentrations. A decrease in flexural strength at the higher concentrations was attributed to an increase in open porosity. © 2008 Wiley Periodicals, Inc. *J Biomed Mater Res Part B: Appl Biomater* 87B: 329–337, 2008

**Keywords:** ceramic; dental/craniofacial material; zirconia; microstructure; strength

## INTRODUCTION

Zirconia stabilized with 3 mol % yttria (3Y-TZP) is currently used in dentistry for the fabrication of crowns, inlays, dental implant abutments, and fixed partial dentures via various CAD/CAM techniques.<sup>1</sup> 3Y-TZP is known to exhibit excellent mechanical properties and biocompatibility.<sup>2–6</sup> It has been used for at least two decades in orthopedics, as femoral heads in total hip replacement.<sup>7,8</sup>

The exceptional mechanical properties of 3Y-TZP rely on the fact that the ceramic is partially stabilized, making possible the mechanism of transformation toughening.<sup>9</sup> Unalloyed zirconia exists under three crystallographic forms. The monoclinic form is stable at room temperature,

the tetragonal form is stable between 1170 and 2370°C, and the cubic form is stable from 2370°C to the melting point ( $2680 \pm 15$ )°C.<sup>10</sup> Various oxides including yttrium oxide can be used to stabilize the tetragonal form at room temperature.<sup>11,12</sup> Zirconia for biomedical applications is commonly stabilized with 3 mol % yttrium oxide (3Y-TZP).<sup>8</sup> The amount of stabilizer has to be controlled carefully as it determines the phase stability or transformability, and mechanical properties of the final product.<sup>10,13</sup> The high strength of 3Y-TZP is derived from the tetragonal to monoclinic stress-induced transformation: under stress, at the crack tip, tetragonal grains transform into the monoclinic form. This transformation is accompanied by an increase in volume thereby closing the crack tip and preventing further crack propagation.<sup>14,15</sup>

The basic color of Y-TZP is opaque white to ivory.<sup>16</sup> Both unalloyed and stabilized forms of zirconia have a high refractive index justifying their use as opacifiers in

Correspondence to: I. L. Denry (e-mail: denry.1@osu.edu)

© 2008 Wiley Periodicals, Inc.

ceramic glazes.<sup>10</sup> In dental restorations, translucent colored porcelain is veneered over the unshaded zirconia core to render esthetics. However, using a shaded zirconia core is thought to lead to better esthetic results, allowing a more natural appearance, similar to the opaque, yellow dentin overlaid by translucent enamel. Two main approaches for coloring zirconia are available. In one technique, metal oxides are mixed with the starting Y-TZP powder before sintering at high temperature, this technique has successfully led to the reproduction of human teeth shades.<sup>3</sup> Another approach currently used for dental restorations involves the infiltration of machined restorations at the pre-sintered stage with chloride solutions of rare earth elements to produce cores of various shades.<sup>17,18</sup> It was shown that the concentration of the coloring solution affected the final shade, while the immersion duration had no significant effect. However, no data on the mechanical properties or resistance to low temperature degradation were reported in either of these studies. Overall, very few reports are available on the mechanical properties and sensitivity to aging of shaded zirconia for dental restorations.<sup>6</sup> The stability of Y-TZP as well as its mechanical properties depends on various factors such as grain size, nature and amount of stabilizer.<sup>8,12</sup> Using coloring metal oxides to obtain various shades in 3Y-TZP dental restorations has the potential to lead to crystallographic and microstructural changes that could in turn affect the mechanical properties of 3Y-TZP. For example, doping with coloring oxides may affect the grain size and render zirconia less stable encouraging the formation of monoclinic zirconia. The purpose of the present study was to investigate the effect of doping with various coloring oxides, currently used to obtain dental shades, on the lattice parameters, microstructure and mechanical properties and aging sensitivity of 3Y-TZP. The hypothesis tested was that doping may affect the lattice parameters, microstructure, mechanical properties, and resistance to low temperature degradation of 3Y-TZP for dental applications.

## MATERIALS AND METHODS

### Specimen Preparation

Zirconia blanks were prepared by cold isostatic pressing of a commercial 3Y-TZP powder (TZ-3YE, Tosoh®), similar to that currently used to manufacture blanks for CAD/CAM dental restorations. The blanks were sliced into discs (20 mm diameter; 2-mm thick) using a low speed wet diamond saw. Specimens were allowed to bench dry at room temperature for 1 week. Cerium chloride (99.5%, Alfa Aesar, Ward Hill, MA) and cerium acetate (99.9%, Alfa Aesar, Ward Hill, MA) were dissolved in distilled water to produce solutions with concentrations of 1, 5, and 10 wt %. Bismuth chloride (99.9%, Alfa Aesar, Ward Hill, MA) shows a poor solubility in water and was therefore dissolved in acetone to produce the same concentrations. Test specimens ( $n = 15$  per group) were immersed for 30 min

in the respective solutions, under constant stirring and in a closed container to prevent evaporation. Homogeneous incorporation of the dopants in the specimens before and after sintering was assessed by careful observation of fractured sections. Specimens were presintered at 800°C for 1 h at a heating rate of 5°C/min. They were then sintered at 1350°C for 2 h at a heating rate of 16°C/min. At the end of the sintering cycle, the specimens were furnace-cooled to room temperature. Control specimens were immersed in distilled water for the same duration and heat treated according to the same schedule.

### Density Measurements

The mean density of the various groups was determined by Archimedes' method using an analytical scale (Mettler-Toledo, Hightstown, NJ). Five readings were taken per specimen ( $n = 3$  per group). Acceptable density values for biomedical grade zirconia are in the range 6.00 g/cm<sup>3</sup> or greater, according to ASTM standard F1873-98.<sup>19</sup>

### Color Parameters

The color parameters ( $n = 5$  per group) were measured using a calibrated colorimeter (Chroma Meter, Minolta Corp. Ramsey, NJ). The calibration was performed using a standard white tile of known  $L^*$ ,  $a^*$ , and  $b^*$  values before each group. Both top and bottom surfaces of each specimen were measured. Average  $L^*$ ,  $a^*$  and  $b^*$  values were used to calculate the color difference ( $\Delta E^*$  value) of each experimental group compared to the control group using the following equation:

$$\Delta E^* = \sqrt{[(\Delta L^*)^2 + (\Delta b^*)^2 + (\Delta a^*)^2]}$$

where  $\Delta L^*$ ,  $\Delta a^*$ , and  $\Delta b^*$  are the differences between the CIE  $L^*$ ,  $a^*$ , and  $b^*$  color parameters of two samples.<sup>20</sup>

### Crystalline Phase Composition

The crystalline phases of the control group and the groups infiltrated with the 10 wt % solutions were analyzed by X-ray diffraction on as-sintered bulk specimens. Scans were performed in the two-theta range 28–65° at a scanning rate of 1 degree per minute. (XDS 2000 diffractometer, Scintag). The lattice parameters were determined by Rietveld refinement. Additionally, scans were performed in the two-theta range 27–32 degrees at a scanning rate of 0.25 degree per minute to detect the formation of the monoclinic phase after low temperature aging.

### Microstructure

The microstructure of the control group and the groups infiltrated with the 10 wt % solutions was investigated by scanning electron microscopy under secondary electron imaging and in ultra high resolution mode (Sirion, FEI

**TABLE I. Mean Density ( $\rho$ ), Modulus of Elasticity ( $E$ ), and Poisson's Ratio ( $\nu$ ) of the Various Groups ( $\pm$ SD)**

Solution	wt %	Density (g/cm <sup>3</sup> )	Modulus of Elasticity (GPa)	Poisson's Ratio ( $\nu$ )
Control		6.072 $\pm$ 0.008 <sup>a</sup>	218.8 $\pm$ 0.9 <sup>a,b</sup>	0.318 $\pm$ 0.001 <sup>a,b,c</sup>
Cerium acetate	1	6.070 $\pm$ 0.010 <sup>a</sup>	213.5 $\pm$ 4.4 <sup>a</sup>	0.314 $\pm$ 0.001 <sup>a,b</sup>
	5	6.077 $\pm$ 0.009 <sup>a</sup>	218.8 $\pm$ 0.4 <sup>b</sup>	0.314 $\pm$ 0.001 <sup>a,b</sup>
	10	6.077 $\pm$ 0.008 <sup>a</sup>	218.4 $\pm$ 1.3 <sup>a,b</sup>	0.315 $\pm$ 0.001 <sup>a,b</sup>
Cerium chloride	1	6.078 $\pm$ 0.004 <sup>a,b</sup>	219.9 $\pm$ 1.6 <sup>b</sup>	0.319 $\pm$ 0.003 <sup>b,c</sup>
	5	6.086 $\pm$ 0.009 <sup>a,b,c</sup>	220.3 $\pm$ 2.6 <sup>b</sup>	0.313 $\pm$ 0.003 <sup>a</sup>
	10	6.097 $\pm$ 0.009 <sup>c</sup>	219.2 $\pm$ 1.3 <sup>b</sup>	0.323 $\pm$ 0.002 <sup>c</sup>
Bismuth chloride	1	6.093 $\pm$ 0.006 <sup>b,c</sup>	220.2 $\pm$ 3.1 <sup>b</sup>	0.316 $\pm$ 0.004 <sup>a,b</sup>
	5	6.118 $\pm$ 0.002 <sup>d</sup>	—	—
	10	6.076 $\pm$ 0.009 <sup>a</sup>	—	—

Identical letters (a, b or c) denote no statistically significant difference at the  $p \leq 0.05$  level.

Company). Specimens were polished to a 1  $\mu$ m finish using a series of abrasives ending with diamond polishing pastes. They were thermally etched at 1250°C, ultrasonically cleaned in ethanol and gold coated prior to SEM examination. Four digital micrographs were taken per specimen. The mean apparent grain size was measured by the lineal intercept method and the real grain size was calculated, assuming nearly equiaxial grains.<sup>19,21</sup>

Open porosity and average pore size were determined by digital image analysis on optical micrographs using the public domain computer software NIH 1.63 (developed at the US National Institute of Health and available on the Internet at <http://rsb.info.nih.gov/nih-image/>).

### Aging Sensitivity

The aging sensitivity was investigated on annealed disc-shaped specimens after aging in an autoclave (137°C, 2 bars) for 10 h. According to previously published studies, 1 h of aging under these conditions represents about 3 years of service *in vivo*.<sup>22,23</sup> The presence (or absence) of monoclinic phase was ascertained by X-ray diffraction as indicated earlier.

### Elastic Constants

The elastic constants were measured by the pulsed ultrasonic velocity method that involves the transit-time measurement of short wave pulses traveling over a known path through the bulk of the specimen. The ratio of the path length to the transit time yields the velocity. The sound velocity in longitudinal mode ( $V_L$ ) and in shear mode ( $V_S$ ) was measured. From these two wave speeds and the density of the material, the modulus of elasticity and Poisson's ratio were calculated.<sup>24</sup>

### Biaxial Flexural Strength

Specimens ( $n = 15$  per group) were tested in biaxial flexure mode with a ball on ring-of-balls fixture at a crosshead speed of 0.5 mm/min with a universal testing machine (Model 4204 Instron, Canton, MA). The maximum radial

and tangential stresses for a specimen under concentric load ( $\sigma_m$ ) are equal and were calculated from the following equation<sup>25,26</sup>:

$$\sigma_m = \frac{3P(1+\nu)}{4\pi t^2} \left[ 1 + 2 \ln(a/b) + \frac{(1-\nu)}{1+\nu} \left[ 1 - \frac{b^2}{2a^2} \right] \frac{a^2}{R^2} \right]$$

where  $P$  = load;  $b$  = radius of uniform loading at center (estimated as  $t/3$ );  $t$  = disc thickness;  $R$  = disc radius;  $a$  = radius of support circle;  $\nu$  = Poisson's ratio.

### Statistical Analysis

The results were analyzed by one-way ANOVA and Tukey's test to detect statistically significant differences. Student's  $t$ -test was performed to detect statistical differences in color ( $\Delta E^*$  values) between the 1, 5, and 10 wt % groups individually. A  $p$ -value of less than 0.05 was considered statistically significant.

The strength data was analyzed using the Weibull model. For each group, the Weibull modulus  $m$  was determined by least-square fitting of a linearized form of the Weibull distribution.<sup>27</sup>

## RESULTS

### Density

The results of the density measurements for the various groups are presented in Table I. The 1 and 5 wt % bismuth chloride groups and the 10 wt % cerium chloride group to had a significantly higher mean density (6.093  $\pm$  0.006 to 6.118  $\pm$  0.002 g/cm<sup>3</sup>) than the control group (6.072  $\pm$  0.008 g/cm<sup>3</sup>). There was no significant difference in the mean density within the cerium acetate series. In the bismuth chloride series, the mean density of the 10 wt % group was significantly lower (6.076  $\pm$  0.009 g/cm<sup>3</sup>) than that of the 1 and 5 wt % groups. The group infiltrated with 5 wt % bismuth chloride exhibited the highest density (6.118  $\pm$  0.002 g/cm<sup>3</sup>). This value was higher than the theoretical density of 3Y-TZP. The density of the 10 wt % cerium chloride group (6.097  $\pm$  0.009 g/cm<sup>3</sup>) was

**TABLE II. Mean Color Differences ( $\Delta E^*$ ) of the Various Groups ( $\pm$ SD)**

	Control	CA 1%	CA 5%	CA 10%
Control	—	2.57 $\pm$ 0.48	8.27 $\pm$ 1.22	9.30 $\pm$ 1.12
CA 1%	2.57 $\pm$ 0.48	—	5.97 $\pm$ 1.19	6.98 $\pm$ 1.13
CA 5%	8.27 $\pm$ 1.22	5.97 $\pm$ 1.19	—	1.15 $\pm$ 1.06
CA 10%	9.30 $\pm$ 1.12	6.98 $\pm$ 1.13	1.15 $\pm$ 1.06	—
	Control	CC 1%	CC 5%	CC 10%
Control	—	7.29 $\pm$ 1.87	9.82 $\pm$ 1.62	12.17 $\pm$ 1.13
CC 1%	7.29 $\pm$ 1.87	—	2.06 $\pm$ 0.36	6.04 $\pm$ 0.98
CC 5%	9.82 $\pm$ 1.62	2.06 $\pm$ 0.36	—	4.05 $\pm$ 0.75
CC 10%	12.17 $\pm$ 1.13	6.04 $\pm$ 0.98	4.05 $\pm$ 0.75	—
	Control	BC 1%	BC 5%	BC 10%
Control	—	2.18 $\pm$ 1.03	12.60 $\pm$ 0.86	14.22 $\pm$ 0.98
BC 1%	2.18 $\pm$ 1.03	—	10.67 $\pm$ 0.83	12.54 $\pm$ 0.97
BC 5%	12.60 $\pm$ 0.86	10.67 $\pm$ 0.83	—	4.12 $\pm$ 1.19
BC 10%	14.22 $\pm$ 0.98	12.54 $\pm$ 0.97	4.12 $\pm$ 1.19	—

CA, Cerium acetate; CC, cerium chloride; BC, bismuth chloride.

significantly higher than that of its 1 and 5 wt % counterparts.

### Color

The results of the color difference ( $\Delta E^*$ ) calculations are presented in Table II. The intersection of a row and a column in the table states the  $\Delta E^*$  value between the two groups. Color differences for all groups when compared with the control group are graphically displayed in Figure 1(A). A perceptible color difference ( $\Delta E^* > 1$ ) was obtained for all groups when compared to the control. The  $L^*$

values of all experimental groups are shown in Figure 1(B). The relationship between  $a^*$  and  $b^*$  values of the various groups is displayed in Figure 2. Within the cerium acetate series, there was a significant difference between the  $\Delta E^*$  values of the 1 wt % ( $2.57 \pm 0.48$ ) compared with the 5 ( $8.27 \pm 1.22$ ) and 10 wt % ( $9.30 \pm 1.12$ ). There was no significant difference found between the 5 and 10 wt %. A similar pattern was observed in the cerium chloride series as well as the bismuth chloride series. Overall, all treatment groups had a more yellow color than the control group (Figure 2).

### Crystalline Phases

Characteristic X-ray diffraction patterns for the control group and the groups infiltrated with 10 wt % solutions are presented in Figure 3(A to D). The lattice parameters are listed in Table III. Only tetragonal zirconia [PDF 50–1089; Figure 3(E)] was found for all groups. All colored specimens showed a slight increase in lattice parameters compared to the 3Y-TZP control group ( $a = 3.605 \pm 0.001$  Å;  $c = 5.177 \pm 0.002$  Å).

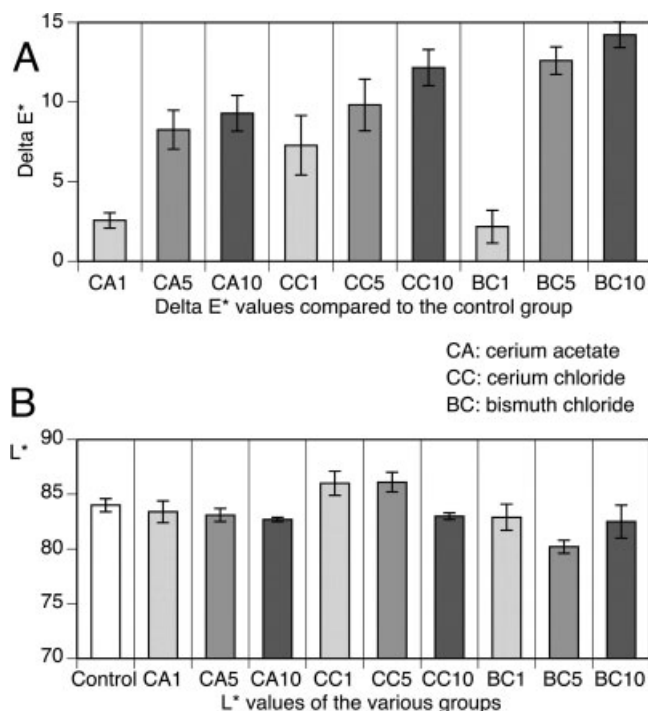


**Figure 1.** Color differences ( $\Delta E^*$ ) for the various groups compared  $L^*$  values of the various groups (B).

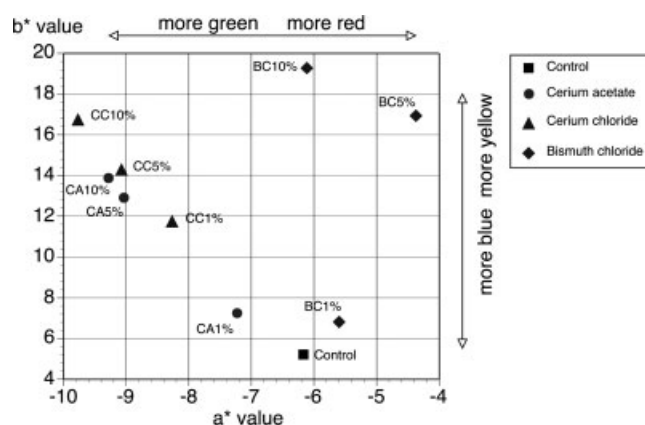


**Figure 2.** Relationship between mean  $a^*$  and  $b^*$  color values of the various groups.

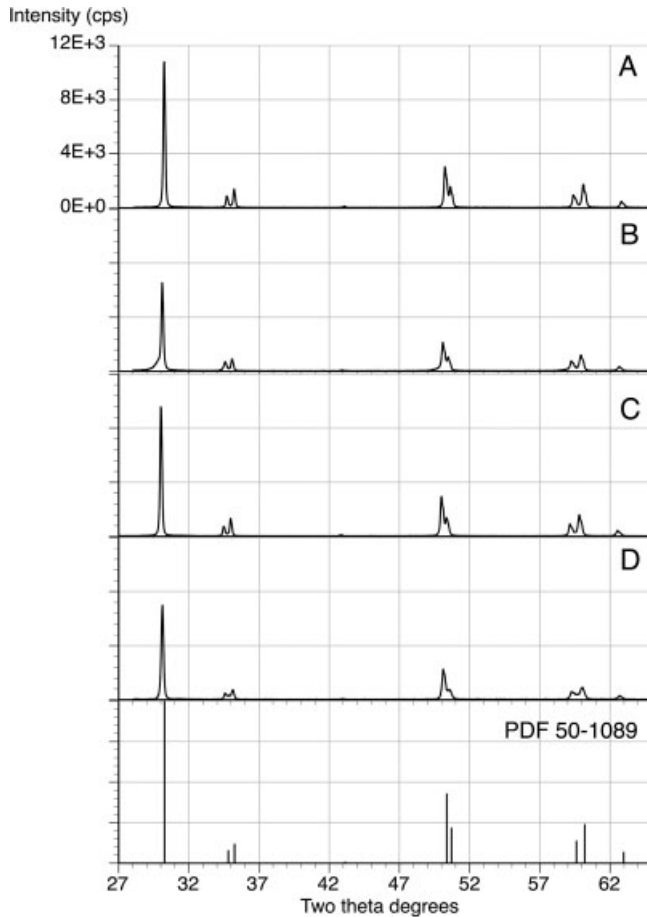


**Figure 3.** X-ray diffraction patterns of the various groups colored with 10 wt % solutions compared with the control group. (A): Control (3Y-TZP); (B): cerium acetate; (C): cerium chloride; (D): bismuth chloride; (E) Tetragonal ZrO<sub>2</sub> - PDF 50-1089.

The group infiltrated with cerium chloride exhibited the largest increase ( $a = 3.613 \pm 0.001 \text{ \AA}$ ;  $c = 5.187 \pm 0.002 \text{ \AA}$ ).

### Microstructure

Representative scanning electron micrographs of the control group and groups infiltrated with the 10 wt % solutions are shown in Figure 4(A–D). The results from grain size measurements are listed in Table III. There was an increase in grain size for all experimental groups compared with the control group ( $0.318 \pm 0.029 \text{ }\mu\text{m}$ ). This increase was statistically significant only for the cerium-infiltrated groups

( $0.350 \pm 0.031$  to  $0.357 \pm 0.035 \text{ }\mu\text{m}$ ;  $p \leq 0.045$ ). Optical micrographs of each group are presented in Figure 5(A–D). The mean open pore size and porosity results are presented in Table III. The bismuth-infiltrated group showed numerous small pores evenly distributed throughout the material [Figure 5(D)] with a total amount of open porosity more than 10 times (1.48%) greater than that of the control group (0.13%). The amount of open porosity for the groups infiltrated with cerium salts was about three times (0.40–0.48%) that of the control group.

### Aging Sensitivity

X-ray diffraction patterns of the various groups before and after aging in autoclave for 10 h are displayed in Figure 6(A–D). There was no detectable amount of monoclinic zirconia in any of the groups after aging.

### Elastic Constants

The results from the elastic constants measurements are summarized in Table I. There were no significant differences between the experimental groups and the control group for either Young's modulus ( $213.5 \pm 4.4$  to  $220.3 \pm 2.6 \text{ GPa}$ ) or Poisson's ratio ( $0.313 \pm 0.003$  to  $0.323 \pm 0.002$ ). Specimens from the groups infiltrated with 5 or 10 wt % bismuth chloride were dome-shaped after sintering. Since grinding the specimens flat would have triggered the stress-induced transformation, testing of the elastic constants and biaxial flexural strength was not performed for these two experimental groups.

### Biaxial Flexural Strength

The mean biaxial flexural strength values with their corresponding standard deviations are graphically displayed in Figure 7. Within the cerium acetate series, the 10 wt % group had significantly lower strength ( $596.0 \pm 196.9 \text{ MPa}$ ) than the control group ( $1087.5 \pm 173.3 \text{ MPa}$ ) or the 1 and 5 wt % groups ( $1101.8 \pm 135.5$  and  $915.1 \pm 85.9 \text{ MPa}$ , respectively). The entire cerium chloride series had a significantly lower flexural strength than that of the control group ( $274.4 \pm 67.3$  to  $860.7 \pm 172 \text{ MPa}$ ). The mean flexural strength of the 1 wt % bismuth chloride group ( $1037.2 \pm 115.3 \text{ MPa}$ ) was not different from that of the control group. For both cerium salt series, the mean flexural strength decreased linearly

**TABLE III.** Mean Lattice Parameters Values ( $\text{\AA}$ ), Grain Size ( $\mu\text{m}$ ) ( $\pm\text{SD}$ ), Open Pore Size ( $\mu\text{m}$ ) ( $\pm\text{SD}$ ) and Open Porosity of the Various Groups

	Cerium Acetate	Cerium Chloride	Bismuth Chloride	Control
Lattice parameter $a$ ( $\text{\AA}$ )	$3.610 \pm 0.001$	$3.613 \pm 0.001$	$3.610 \pm 0.003$	$3.605 \pm 0.001$
Lattice parameter $c$ ( $\text{\AA}$ )	$5.183 \pm 0.002$	$5.187 \pm 0.002$	$5.180 \pm 0.005$	$5.177 \pm 0.002$
Grain size ( $\mu\text{m}$ )	$0.350 \pm 0.031^a$	$0.357 \pm 0.035^a$	$0.349 \pm 0.021^{a,b}$	$0.318 \pm 0.029^b$
Open pore size ( $\mu\text{m}$ )	$26.6 \pm 11.6$	$21.2 \pm 9.2$	$17.2 \pm 10.5$	$18.4 \pm 11.6$
Open porosity (%)	0.48	0.40	1.48	0.13

Identical letters (a, b or c) denote no statistically significant difference at the  $p \leq 0.05$  level.



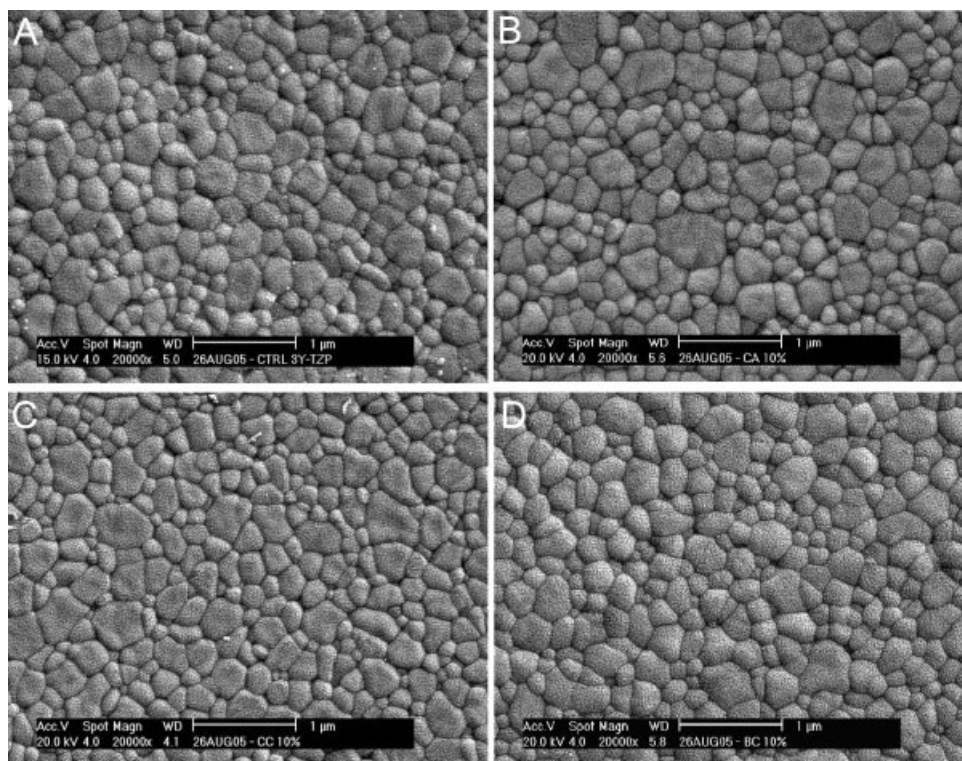


**Figure 4.** Scanning electron micrographs of the various groups colored with 10 wt % solutions compared to the control group. (A): Control (3Y-TZP); (B): cerium acetate; (C): cerium chloride; (D): bismuth chloride. (bar = 1  $\mu$ m)

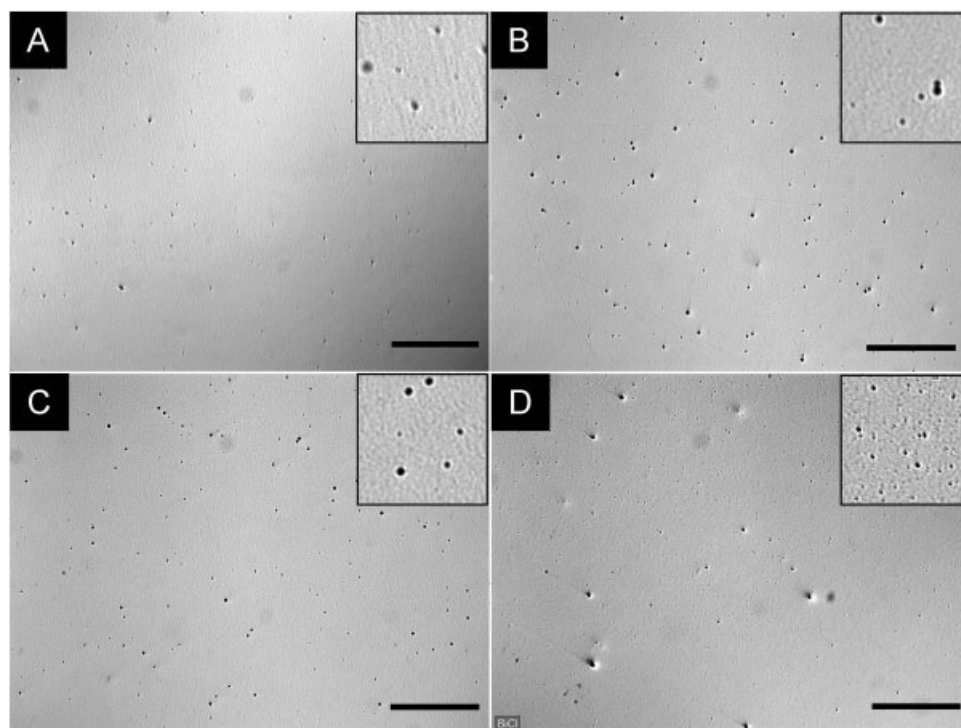


**Figure 5.** Optical micrographs of the various groups colored with 10 wt % solutions compared with the control group, showing various amounts of open porosity. (A): Control (3Y-TZP); (B): cerium acetate; (C): cerium chloride; (D): bismuth chloride (bar = 1 mm). Square in upper right corner shows higher magnification ( $0.5 \times 0.5$  mm<sup>2</sup>).

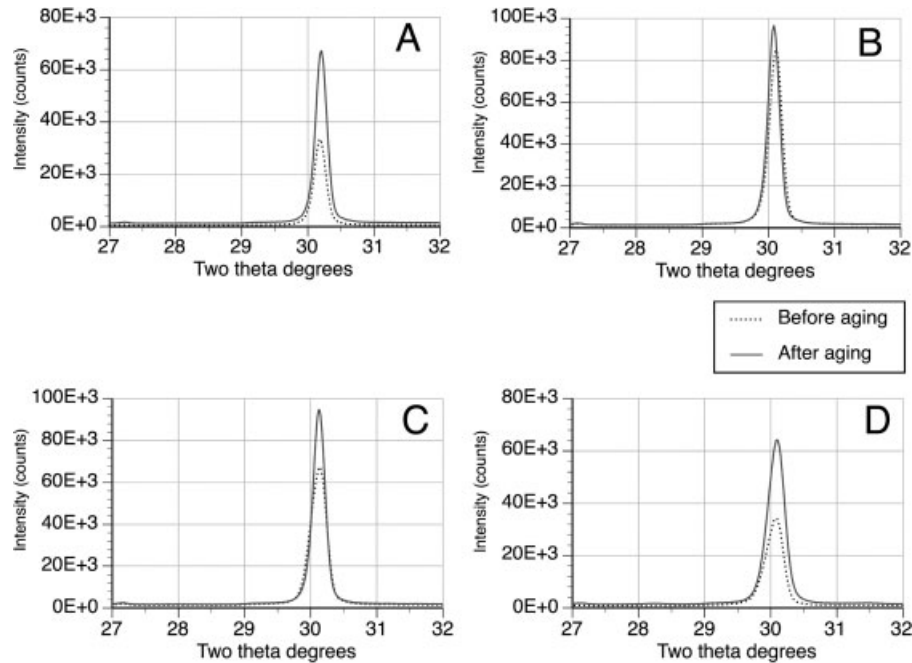


**Figure 6.** X-ray diffraction patterns of the various groups colored with 10 wt % solutions compared to the control group before and after aging in autoclave for 10 h ( $\text{CuK}\alpha = 1.5406 \text{ \AA}$ ). (A): Control (3Y-TZP); (B): cerium acetate; (C): cerium chloride; (D): bismuth chloride. Dashed line: before aging. Solid line: after aging.

( $R^2 > 0.95$ ) with increasing concentration. The Weibull analyzes for the various groups are shown in Figure 8. The 1 and 5 wt % cerium acetate groups and the 1 wt % bismuth chloride group had a similar or higher Weibull modulus (7.04–10.06) than the control group (6.13). The entire cerium chloride series as well as the 10 wt % cerium acetate group had a low reliability with a Weibull modulus of less than 4.45.

## DISCUSSION

The present study aimed at evaluating the effects of cerium and bismuth as dopants on the phase composition, color and flexural strength of 3Y-TZP. A dopant is classically defined as an element incorporated in trace amounts to alter

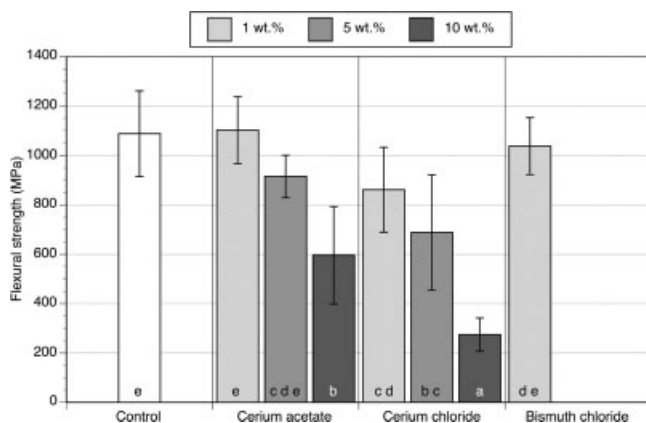


**Figure 7.** Mean biaxial flexural strength of the various groups (identical letters denote no statistically significant difference at  $p \leq 0.05$  level).

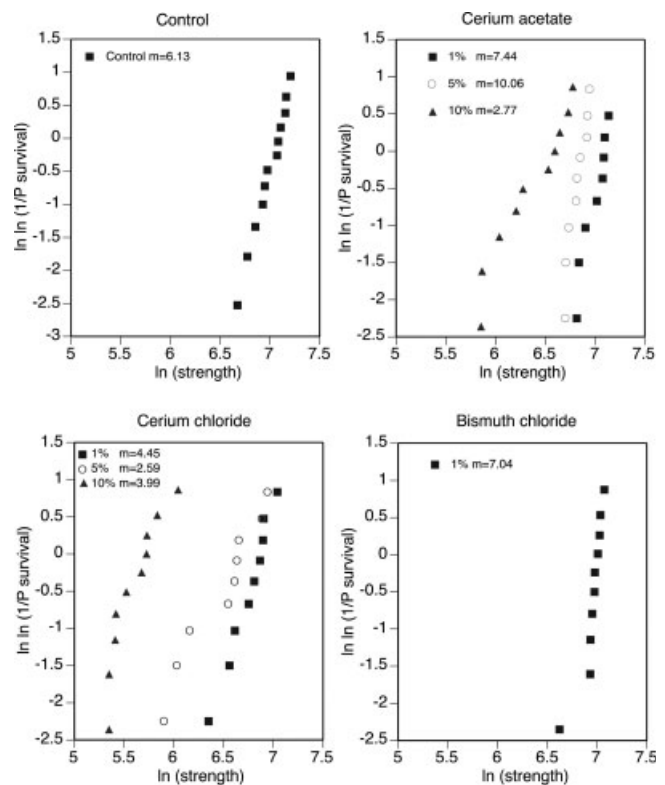


**Figure 8.** Weibull plots and Weibull modulus of the various experimental groups.

the chemical properties. Dopants are present in zirconia either as a distinct phase or as a solid solution. It is well established that dopants such as silica or alumina directly influence the grain morphology, microstructure and stability of zirconia.<sup>28–30</sup> Various other elements have been used as dopants in an attempt to improve the phase stability and prevent the low temperature aging process of Y-TZP in the presence of water. Ceria has been shown to act as a sintering aid and increase grain size<sup>31</sup> while improving the aging resistance.<sup>32,33</sup> Bismuth can act as a stabilizer and sintering aid for tetragonal zirconia<sup>34,35</sup> The results of the present study confirmed that there was a significant increase in grain size in the cerium-infiltrated groups. There was also a slight increase in grain size in the bismuth-infiltrated group, although not significant.

The presence of additional metal ions was also expected to modify the lattice parameters of 3Y-TZP. Our results showed that only the tetragonal phase was present in all groups after sintering at 1350°C for 2 h. The values obtained for the lattice parameters of the control 3Y-TZP material ( $a = 3.605 \text{ \AA}$ ;  $c = 5.177 \text{ \AA}$ ) compared well with published values ( $a = 3.606 \text{ \AA}$ ;  $c = 5.176 \text{ \AA}$ ).<sup>28</sup> There was a slight increase in lattice parameters for all doped groups, corresponding to a moderate increase in unit cell volume (between 0.4 and 0.7 vol %). These results indicate that if solid solutions of cerium or bismuth in 3Y-TZP were formed, they only involved very small quantities that were not detectable by X-ray diffraction. In addition, no noticeable change in grain shape, dihedral angles, or grain boundary geometry was observed between the control and doped groups. This points toward the absence of vitreous phase at triple joints for both bismuth and cerium-doped groups.<sup>28,36</sup>

The density results were comprised between 99.5 and 100.3% of the theoretical density for all groups, thereby seemingly indicating a proper sintering protocol. However, the addition of a dopant with higher atomic weight in the zirconia matrix is likely to cause a progressive change in the density of the final product depending on the amount of dopant incorporated.<sup>37</sup> In the present study, zirconium with an atomic weight of 91.22 could have been replaced by cerium (140.12) or bismuth (208.98) leading to a subsequent increase in density. This is further supported by the fact that the true density values were even higher than those reported due to the presence of pores. The open porosity of the groups infiltrated with the 10 wt % cerium salt solutions was greater than the value suggested by ASTM standard F1973-98<sup>19</sup> (0.1 vol %). Moreover, the open porosity of the group infiltrated with bismuth chloride reached 1.48% with a smaller average pore size. Optical microscopy revealed that these pores were more spherical than polyhedral. This, together with the very small average pore size indicates that these pores could be caused by the volatilization of a chemical or solvent. The melting point for bismuth chloride is 447°C, it is therefore possible that the observed residual porosity be due to the transformation of bismuth chloride.

In addition, bismuth chloride in concentrations of 5 or 10 wt % had a detrimental effect on the sintering behavior of the final product. It is possible that the convex dome-shape of the sintered specimens in these two groups be due to the evaporation of acetone, leading to an increased dopant concentration on the top surface of the discs together with better sintering. This would also explain the deeper chroma observed on the same surface compared to the bottom surface. This problem did not occur in the 1 wt % group due to the lower concentration of bismuth in the overall solution.

The flexural strength of the control group compared well with previously reported values.<sup>4,5,38,39</sup> The decrease in flexural strength for the groups infiltrated at the highest concentrations could be due to the observed increase in grain size.<sup>40</sup> However, this increase was very moderate and it seems more likely that the presence of porosity was the determining factor since pores are known to act as crack initiators.<sup>31,41</sup> There was a linear relationship between the pore size and the flexural strength for the two groups infiltrated with the 10 wt % cerium salts and the control group ( $R^2 = 0.97$ ). The Weibull modulus of the experimental groups as well as the control group were lower than published values.<sup>5,38,39</sup> However, differences in specimen preparation, specimen size, sintering temperature, and type of test are likely to contribute to differences in Weibull moduli and the overall reliability of the material.

Coloring 3Y-TZP with either cerium or bismuth solutions up to 10 wt % did not affect the resistance to low temperature aging, which was excellent for both unshaded controls and colored groups with no detectable amount of monoclinic zirconia after aging in autoclave for 10 h.

Cerium and bismuth salts did have an effect on the color properties of 3Y-TZP. In both cerium series, the  $a^*$  values decreased and the  $b^*$  values increased linearly as the cerium concentration increased, leading to a deeper cream color compared with the control group. The bismuth series showed more changes in  $b^*$  values than  $a^*$  values one, leading to the deeper orange color than the cerium series. These results were in good agreement with previous studies.<sup>3,18</sup>

## CONCLUSIONS

Coloring 3Y-TZP with cerium acetate solutions up to 5 wt % yielded a favorable shade while not affecting the mechanical properties significantly. Higher concentrations led to a significant decrease in flexural strength with no further significant change in  $\Delta E^*$  values. Coloring with cerium chloride was most efficient, leading to higher  $\Delta E^*$  values than cerium acetate or bismuth chloride. However, it also led to a significant decrease in flexural strength even for concentrations as low as 1%. Coloring with bismuth chloride is possible at low concentrations of 1% or less without adverse effects on flexural strength. The resistance to low temperature degradation was not affected by any of the coloring solutions tested.



## REFERENCES

- Denry I, Kelly JR. State of the art of zirconia for dental applications. *Dent Mater* 24:299–307.
- Filser F, Kocher P, Gauckler LJ. Net-shaping of ceramic components by direct ceramic machining. *Assembly Autom* 2003; 23:382–390.
- Cales B. Colored zirconia ceramics for dental application. *Bioceramics* 1998;11:591–594.
- Guazzato M, Albakry M, Ringer SP, Swain MV. Strength, fracture toughness and microstructure of a selection of all ceramic materials. II. Zirconia-based dental ceramics. *Dent Mater* 2004;20:449–456.
- Kosmac T, Oblak C, Jevnikar P, Funduk N, Marion L. Strength and reliability of surface treated Y-TZP dental ceramics. *J Biomed Mater Res* 2000;53:304–313.
- Ardlin B. Transformation-toughened zirconia for dental inlays, crowns and bridges: Chemical stability and effect of low-temperature aging on flexural strength and surface structure. *Dent Mater* 2002;18:590–595.
- Calès B, Stefani Y, Lilley E. Long-term *in vivo* and *in vitro* aging of a zirconia ceramic used in orthopaedy. *J Biomed Res* 1994;28:619–624.
- Piconi C, Macauro G. Zirconia as a ceramic biomaterial. *Biomaterials* 1999;20:1–25.
- Kelly JR, Denry I. Stabilized zirconia as a structural material. *Dent Mater* 24:289–298.
- Subbarao EC. Zirconia-an overview. In: Heuer AH, Hobbs LW, editors. *Science and Technology of Zirconia*. Columbus, OH: The American Ceramic Society; 1981. pp 1–24.
- Gupta TK, Bechtold JH, Kuznicki RC, Cadoff LH, Rossing BR. Stabilization of tetragonal phase in polycrystalline zirconia. *J Mater Sci* 1977;12:2421–2426.
- Gupta TK, Lange FF, Bechtold JH. Effect of stress-induced phase transformation on the properties of polycrystalline zirconia containing metastable tetragonal phase. *J Mater Sci* 1978;13:1464–1470.
- Chevalier J. What future for zirconia as a biomaterial? *Biomaterials* 2006;27:535–543.
- Garvie RC, Hannink RH, Pascoe RT. Ceramic steel? *Nature* 1975;258:703–704.
- Heuer AH. Transformation toughening in  $ZrO_2$ -containing ceramics. *J Am Ceram Soc* 1987;70:689–698.
- Lee DY, Kim DJ, Song YS. Chromaticity, hydrothermal stability, and mechanical properties of t- $ZrO_2/Al_2O_3$  composites doped with yttrium, niobium, and ferric oxides. *Mat Sci Eng A* 2000;289:1–7.
- Kulkarni NK, Sampath S, Venugopal V. Studies on stabilised zirconia as host phase for the fixation of actinides, rare-earths and sodium. *Ceram Int* 2001;27:839–846.
- Suttor D, Hauptmann H, Schnagl R, Frank S, inventors; 3M Espe AG, assignee. Coloring ceramics by way of ionic or complex-containing solutions. U.S. Pat. 6,709,694; 2004.
- ASTM. Standard Specification for High-Purity Dense Ytria-Tetragonal Zirconium Oxide Polycrystal (Y-TZP) for Surgical Implant Applications. *Annual Book of ASTM Standards*, ASTM. West Conshohocken: ASTM; F1873-98. Vol. 13.01; 2004. pp 1381–1383.
- Craig RG. *Restorative Dental Materials*, 12th ed. St Louis: Mosby Company; 2006.
- ASTM. Standard Test Methods for Determining Average Grain Size. *Annual Book of ASTM Standards*, E112-96 ASTM. West Conshohocken: ASTM; Vol. 3.01. 2003. pp 243–266.
- Chevalier J, Calès B, Drouin JM. Low-temperature aging of Y-TZP ceramics. *J Am Ceram Soc* 1999;82:2150–2154.
- Deville S, Chevalier J, Grémillard L. Influence of surface finish and residual stresses on the ageing sensitivity of biomedical grade zirconia. *Biomaterials* 2006;27:2186–2192.
- ASTM. Standard Practice for Measuring Ultrasonic Velocity in Materials. *Annual Book of ASTM Standards*. West Conshohocken: ASTM; E 494-95; 1995.
- Shetty DK, Rosenfield AR, McGuire P. Biaxial fracture tests for ceramics. *Ceram Bull* 1980;59:1193–1197.
- Wachtman JBJ, Capps W, Mandel J. Biaxial flexure testing of ceramic substrates. *J Mater* 1972;7:188–194.
- Wachtman JB. *Mechanica properties of ceramics*, 1st ed. New York: Wiley; 1996.
- Grémillard L, Epicier T, Chevalier J, Fantozzi G. Microstructural study of silica-doped zirconia ceramics. *Acta Mater* 2000;48:4647–4652.
- Mecartney M. Influence of an amorphous second phase on the properties of yttria-stabilized tetragonal zirconia polycrystals (Y-TZP). *J Am Ceram Soc* 1987;70:54–58.
- Tsubakino HNR, Hamamoto M. Effect of alumina addition on the tetragonal-to-monoclinic phase transformation in zirconia-3 mol % Ytria. *J Am Ceram Soc* 1991;74:440–443.
- Boutz MMR, Winnubst AJA, van Langerak B, Olde Scholtenhuis RJM, Kreuwel K, Burggraaf AJ. The effect of ceria codoping on chemical stability and fracture toughness of Y-TZP. *J Mater Sci* 1995;30:1854–1862.
- Hernandez MT, Jurado JR, Duran P, Fierro JLG. Subeutectoid degradation of yttria-stabilized tetragonal zirconia polycrystal and ceria-doped yttria-stabilized tetragonal zirconia polycrystals ceramics. *J Am Ceram Soc* 1991;74:1254–1258.
- Duh JG, Lee MY. Fabrication and sinterability in  $Y_2O_3-CeO_2-ZrO_2$ . *J Mater Sci* 1989;24:4467–4474.
- Keizer K, Burggraaf AJ, de With G. The effect of  $Bi_2O_3$  on the electrical and mechanical properties of  $ZrO_2-Y_2O_3$  ceramics. *J Mater Sci* 1982;17:1095–1102.
- Gulino A, La Delfa S, Fragala I, Egdel RG. Low-temperature stabilization of tetragonal zirconia by bismuth. *Chem Mater* 1996;8:1287–1291.
- Ikuhara Y, Thavorniti P, Sakuma T. Solute segregation at grain boundaries in superplastic  $SiO_2$ -doped TZP. *Acta Mater* 1997;45:5275–5284.
- Corradi AB, Bondiolo F, Ferrari AM. Role of praseodymium on zirconia phases stabilization. *Chem Mater* 2001;13:4550–4554.
- Kosmac T, Oblak C, Jevnikar P, Funduk N, Marion L. The effect of surface grinding and sandblasting on flexural strength and reliability of Y-TZP zirconia ceramic. *Dent Mater* 1999; 15:426–433.
- Guazzato M, Quach L, Albakry M, Swain MV. Influence of surface and heat treatments on the flexural strength of Y-TZP dental ceramic. *J Dent* 2005;33:9–18.
- Quinn JB, Sundar V, Lloyd IK. Influence of microstructure and chemistry on the fracture toughness of dental ceramics. *Dent Mater* 2003;19:603–611.
- Luo J, Stevens R. Porosity-dependence of elastic moduli and hardness of 3Y-TZP ceramics. *Ceram Int* 1999;25:281–286.